

Phoswitch Gamma Ray Detector for CubeSat Applications

Scott Candey

May 15th, 2020

Abstract

A simple phoswitch gamma ray detector has been designed and simulated to demonstrate a possible implementation using small blocks of various common gamma ray scintillators. This project is intended in part to prove the effectiveness of silicon photomultipliers (SiPMs) for SmallSat or CubeSat instrumentation applications as a continuation of summer work at NASA Goddard Space Flight Center (NASA GSFC) with Dr. Georgia de Nolfo. The design was built at Swarthmore College with adviser Professor Lynne Molter, though lab testing has been delayed. Simulations were based on values from a review of relevant literature, focusing on gamma ray detector analysis in MEGAlib and GEANT4. Pulse shape modeling was also attempted for depicting the phoswitch aspect of the detector. While lab testing with radiation sources is required, simulations and literature review demonstrate that the basic concept is sound and worthy of continued research.

Contents

1	Motivation	2
2	Background	3
2.1	Gamma ray detection	3
2.2	Gamma ray interactions	4
2.3	Phoswitch detector	5
2.4	Pulse Modeling	7
3	Instrument design	9
4	Results	11
4.1	Experimental design	11
4.2	Expected results	11
5	Simulation	12
6	Conclusion	14
7	Acknowledgements	15
	References	15
	Appendices	17
A	Materials	17
A.1	Cost	17
A.2	Bill of Materials	17
B	Radiation sources	18
C	MEGAlib Code	18
C.1	MEGAlib Geometry file	18
C.2	MEGAlib Source file	22

1 Motivation

Neutral particle measurement provides scientists a window into our own Sun and astronomical processes that compliments measurement through other methods. Neutral particles, unhindered by magnetic fields, provide a direct measure of their source whether terrestrial, solar, or astrophysical. Gamma rays, high energy photons, are often associated with particle physics interactions and can provide hints about solar activity, supernova, or even black hole collisions.

Simple gamma ray detectors consist of a plastic or crystal scintillator and a photo detector. The work completed over my summer internship with Dr. Georgia de Nolfo at NASA Goddard Space Flight Center focused on replacing photomultiplier tube (PMT) detectors with silicon photomultiplier (SiPM) designs for low voltage and footprint applications on shoebox-sized satellites called CubeSats. Figure 1 shows a render of the TRYAD CubeSat, which uses SiPM-based gamma ray detectors to study terrestrial gamma rays from low earth orbit.[1]

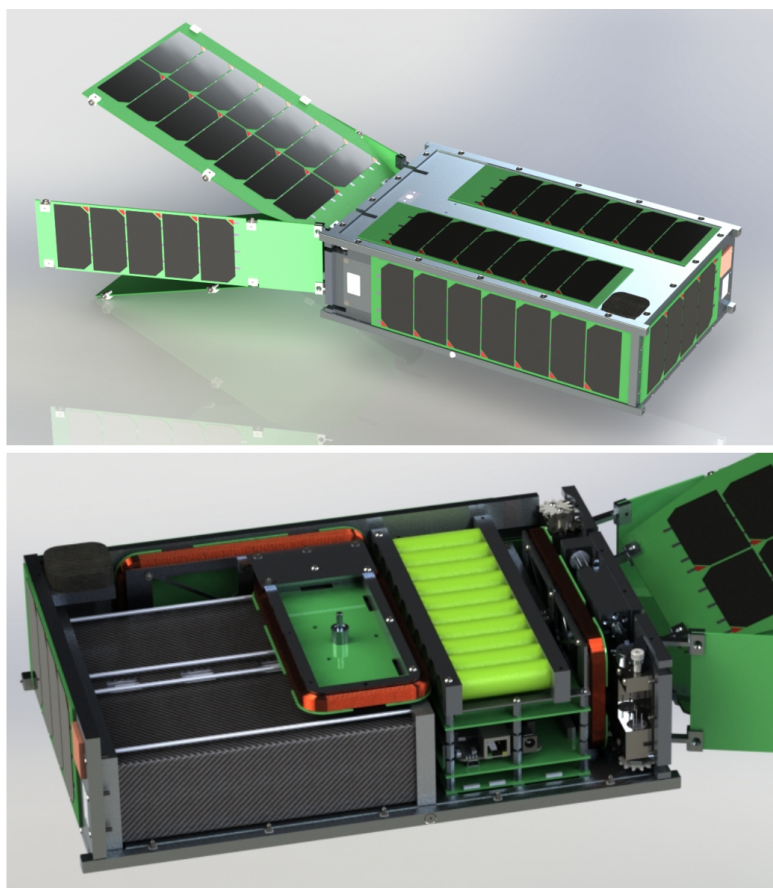


Figure 1: Render of TRYAD CubeSat

These relatively cheap satellites could be put into low-Earth orbit to study the Sun's interactions with the Earth's magnetic field and atmosphere. Space weather like solar flares, coronal

mass ejections, and solar wind consists primarily of high energy particles with both charged and neutral particles being shot out of the sun. Auroras are the most notable result of interactions with Earth's magnetic fields and atmosphere, but intense solar storms can lead to increased radiation dosages for astronauts on the ISS, cause issues with GPS or telecommunications satellites, or even potentially damage our power grid with the long high voltage power lines acting like antennae. More extensive gamma ray detection in low earth orbit would improve space weather modeling and the quality of solar storm predictions.

CubeSats have also been proposed to study the Sun or other planets up close, where many smaller satellites may be more resilient than one large satellite. In all of these applications, a very small gamma ray detector would be a good addition to a primary instrument for expanding our understanding of the Sun's influences on our solar system.

2 Background

2.1 Gamma ray detection

Gamma rays are simply high energy photons. Any photons with energy higher than X-rays are considered gamma rays, ranging from roughly 10 kilo electron volts (keV) to over 100 tera electron volts (TeV). Like X-rays, gamma rays pass through most materials without interacting with them very much. This property is what allows X-rays to be used to look inside the human body. With the wavelength of X-rays on the order of the size of an atom, they are likely to pass between atoms of a material. X-rays are less likely to interact with the softer, less dense tissues and more likely to interact with bone so bones cause dark areas on X-ray sensitive film. Figure 2 shows some common objects for context of wavelength in the electromagnetic spectrum.

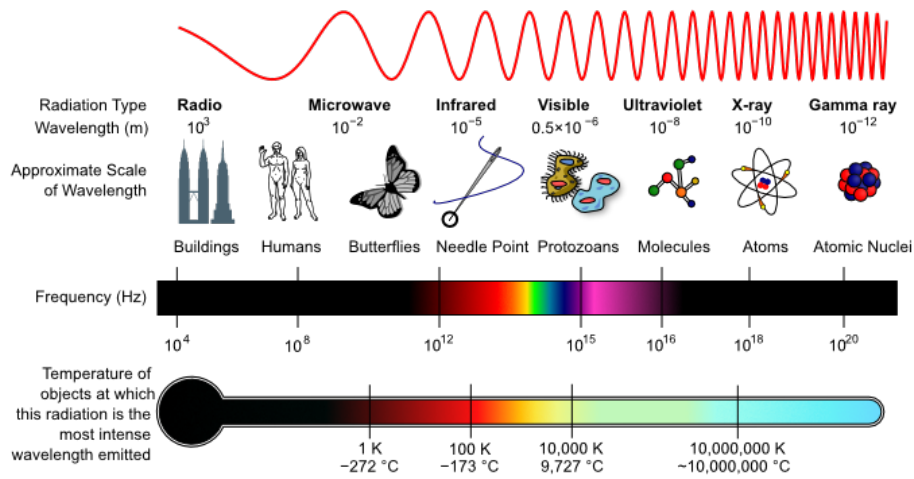


Figure 2: Electromagnetic Spectrum

Gamma rays are very unlikely to interact with any sort of thin film, so blocks of plastic or crystal is needed to cause interactions. When a gamma ray enters one of these blocks, the material scintillates, or releases lower energy photons through various particle physics methods. By collecting the photons due to scintillation in a photodetector like a SiPM, the energy of the original gamma ray can be measured. This simple detector can actually be built in the lab for \$100, as designed by the Cosmic Watch project.[2]

The main issue with using this simple detector design for gamma ray detection is charged particles will interact much more frequently compared to gamma rays. In particular, cosmic ray muons easily drown out the signals due to the target gamma rays. In the Cosmic Watch project, researchers are attempting to measure the general category of cosmic rays, so there is no issue with mixing the types of particles for their goal.

2.2 Gamma ray interactions

Low and medium energy gamma rays primarily interact with scintillating materials through the photoelectric effect and Compton scattering. Pair production is the third way gamma rays interact with scintillators, but for the target gamma rays with energies under 1 mega electron volt (MeV), the photoelectric effect and Compton scattering interactions dominate.

The photoelectric effect occurs when a gamma ray interacts with a scintillator atom and an electron is emitted with the same energy as the incident gamma ray. This photoelectron moves through the material, ionizing other atoms so that new photons are produced when the atoms return to ground state. The energy of the photons produced is proportional to the energy of the

incident gamma ray.

Compton scattering occurs when a gamma ray hits an electron in the scintillator material, transferring some amount of energy to the electron and flying off with lower energy at a different angle. Depending on the outgoing angle, the gamma ray can transfer a range of energies proportional to the incident energy, described by the Compton scattering equation.[3] The minimum energy transferred is simply none, but the maximum energy transferred is related to the frequency of the incident gamma ray in proportion to the rest mass of the particle, in this case an electron. For a 662 keV gamma ray as produced by a Cesium-137 source, a source which is commonly used for detector calibration, the maximum energy imparted to an electron is 477 keV.

When observing these features on a distribution of energies in a real detector, the photoelectric effect interactions are displayed as a Gaussian peak called a photopeak, with variation around the energy of the incoming gamma rays. The theoretical photopeak would be an impulse, precisely at the energy of the incident gamma rays. Compton scattering interactions are displayed as a dip and a smooth edge, though the theoretical Compton edge is very sharp. A demonstration of the difference between a theoretical edge and a realistic representation is shown in Figure 3 using p-terphenyl plastic scintillator, which has a particularly strong Compton scattering response.

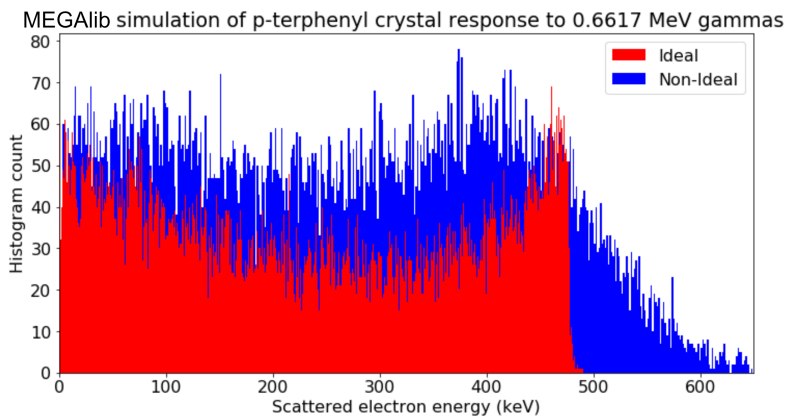


Figure 3: MEGALib simulation of p-terphenyl scintillator with 662 keV gamma rays in ideal and realistic detectors

2.3 Phoswitch detector

The phoswitch detector is a compound detector design that attempts to differentiate gamma rays from charged particles using two different plastic or crystal scintillators read out together

by photodetectors like SiPMs. The pulses due to incoming gamma rays or other particles vary between the two materials so pulse shape discrimination can be used to obtain the energy of the gamma rays and other particles without extensive shielding or separate anti-coincidence detectors. [4]

The basic phoswitch concept has been used with photomultiplier tubes to improve gamma scintillation cameras used in medicine along with some usage in space physics. [5] [6] Most phoswitch detectors use a combination of a large scintillating crystal that has a slow response to incoming particles with a thin plastic scintillator with a fast response. [7] [8]

The pulses from two different materials will have different peak heights and decay times, with plastic scintillators having much a much faster decay time compared to most crystal scintillators. In any low or medium energy gamma ray interaction in a scintillator, some particle physics interaction like Compton scattering or the photoelectric effect occurs and leaves an electron moving through the material. In inorganic crystal scintillators, the moving electron creates electron-hole pairs, which migrate through the crystal until they excite a activation site. The activation site, made of a different element than the crystal itself, takes a relatively long time to transition back to the ground state, but releases many photons in the visible spectrum when it does. Those photons are then captured by the silicon photomultipliers. Plastic scintillators fall into a category of organic scintillators, where specially designed molecules of the scintillator are directly excited by the passing electron and quickly return to ground state, producing photons in selected wavelengths much faster than crystals. If the selected wavelength is outside the visible spectrum, an added waveshifter material absorbs UV photons and reemits them as blue or green photons.[9]

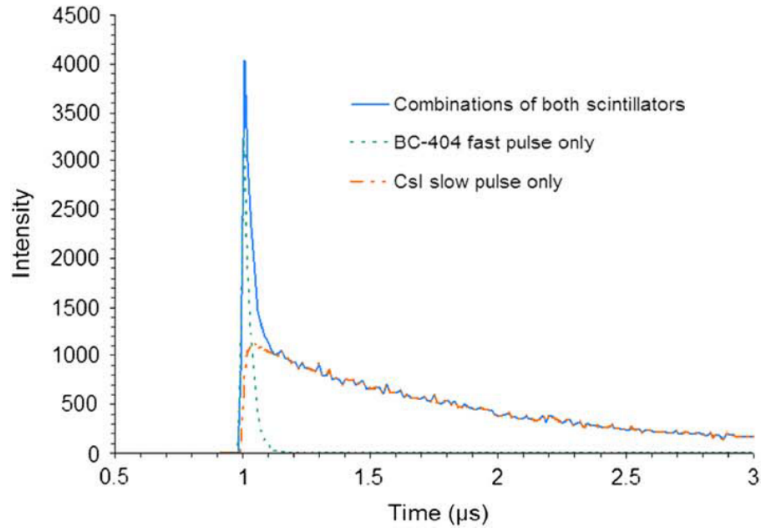


Figure 4: Example of phoswitch detector pulses from PhosWatch project

Gamma rays do not often interact with low density material like plastic, so when a signal appears in both the fast and slow scintillator that signal is likely due to a charged particle like a cosmic ray muon. By removing the coincidence events, the energy distribution of the gamma rays alone can be determined. Figure 4 shows an example of a coincidence event with fast response of a plastic BC-404 scintillator combined with the slow response from a crystal CsI scintillator from the PhosWatch nuclear nonproliferation detector project.[10]

The PhosWatch detector uses pulse shape discrimination to identify interacting particles by measuring pulse heights and other characteristics like rise time and decay time.

2.4 Pulse Modeling

Without oscilloscope data to enable reasonable simulations, demonstrating the expected voltage pulses for this detector is difficult. An attempt to generate artificial data reminiscent of expected results is described below. Detector pulses have a rapid rise time and slower fall time which are already characterized for some of the scintillator materials utilized.[11] [12] For detectors with relatively thin scintillators on silicon photomultipliers, the energy deposited in the scintillator (and therefore measured by the SiPMs) by a charged particle is roughly described by a Landau distribution.[9] The sum of the areas under many pulses is also described by a Landau distribution, though it should be convolved with a Gaussian distribution to account for thermal noise in the detector system.[13] For a gamma ray detector, this distribution represents energy loss of an electron moving through a thin scintillator. The model in Figure 5 demonstrates a possible

coincidence pulse similar to the example from the PhosWatch detector, with decay times representative of scintillator materials chosen for this project. The Landau distribution was used in this case to approximate the shape of the pulse, but the distribution does not represent an actual experimental distribution of voltage over time.

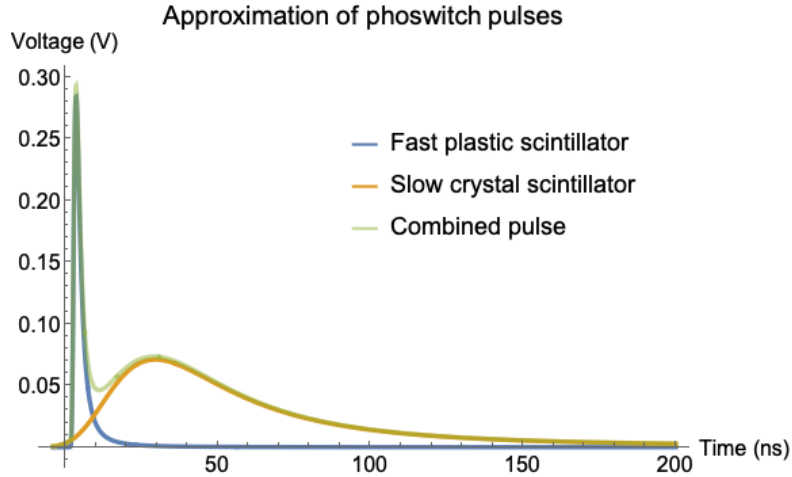


Figure 5: Model of fast plastic and slow crystal responses using Landau distribution

Individual voltage pulses can be analyzed to approximate the energy deposited in the scintillator by an incident particle. Figure 6 demonstrates another rough approximation of a fast plastic pulse with the peak height and decay time measured. Measuring pulse heights alone provides a reasonable approximation of the energy deposited in the detector after calibration, but voltage pulses can also be integrated over time and divided by the known resistance and amplification to estimate the charge in the SiPMs due to each incident particle. The decay time and pulse height can also be used in a phoswitch detector or a single scintillator detector to determine the type of particle that interacted with the detector.

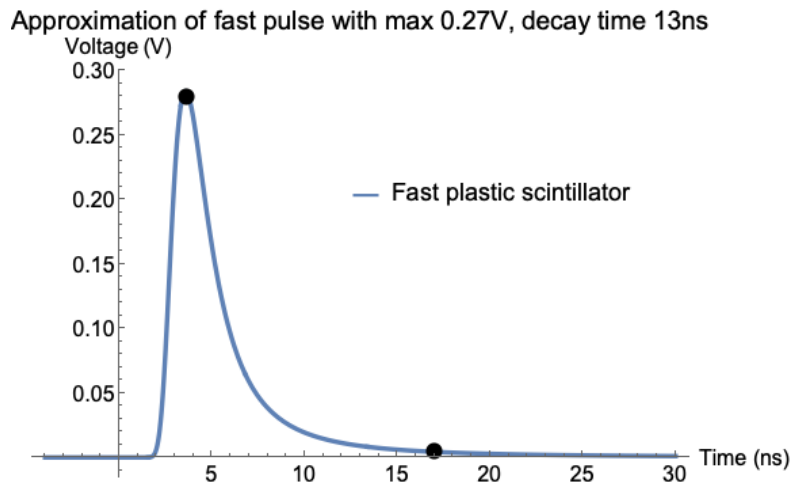


Figure 6: Model of fast plastic pulse using Landau distribution with measurements

In developing this pulse model, a Gaussian distribution was considered to represent electronic and thermal noise in the detector system. A Landau distribution numerically convolved with a Gaussian distribution would fit real or simulated pulses better, but for the purposes of demonstrating pulse shapes, the significantly increased computation time is not needed. An example of the convolved shape is shown in Figure 7.

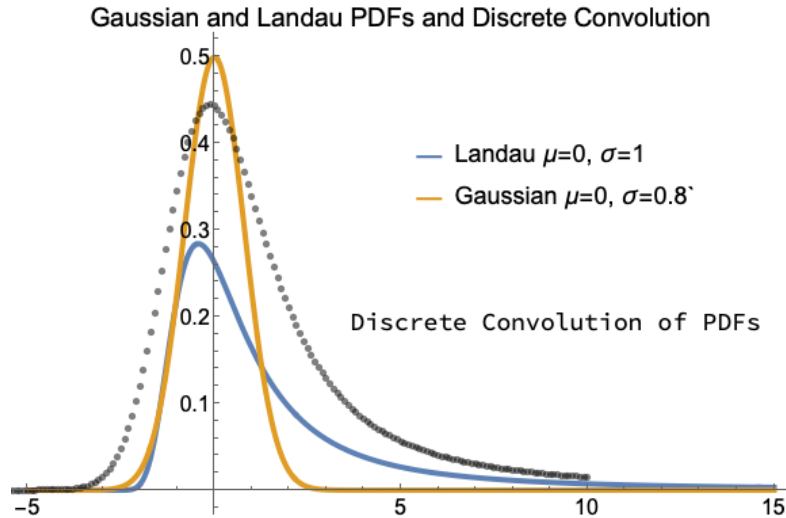


Figure 7: Landau distribution numerically convolved with Gaussian distribution

In order to obtain measurable voltage pulses during experimentation, photodetectors and scintillators were sized to easily measure a range of small laboratory radiation sources.

3 Instrument design

My detector design consisted of two 24mm x 24mm x 12mm scintillators Teflon-taped together resting on a bed of 16 standard Hamamatsu SiPMs. In order to find the optimal combination of scintillating materials for this simple phoswitch detector application, I intended to do experimental trials with standard scintillating materials such as BGO crystal, CsI(Tl) crystal, and EJ-212 plastic. I also purchased EJ-240 plastic, which has a slower response than EJ-212 plastic but faster than the crystals. Figure 8 shows purchased components assembled out of the dark box. The SiPMs are on the left side of the circuit board, with dots in the middle. The white block on the right is the plastic scintillator wrapped in Teflon tape. The circuit board underneath powers the SiPMs, converts SiPM charge to a voltage pulse and amplifies and shapes the voltage pulse to be read out by an oscilloscope.

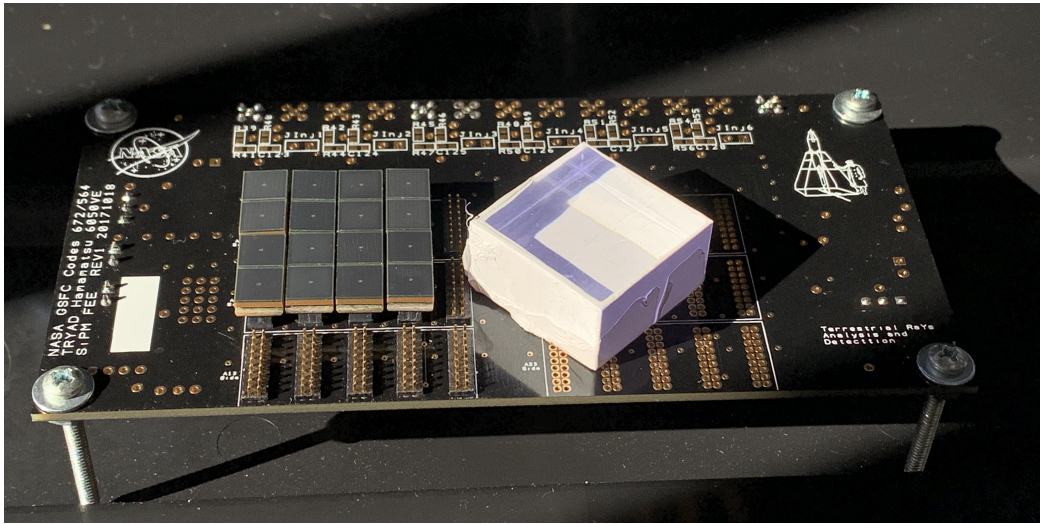


Figure 8: Image of SiPMs and board with wrapped EJ-212 scintillator

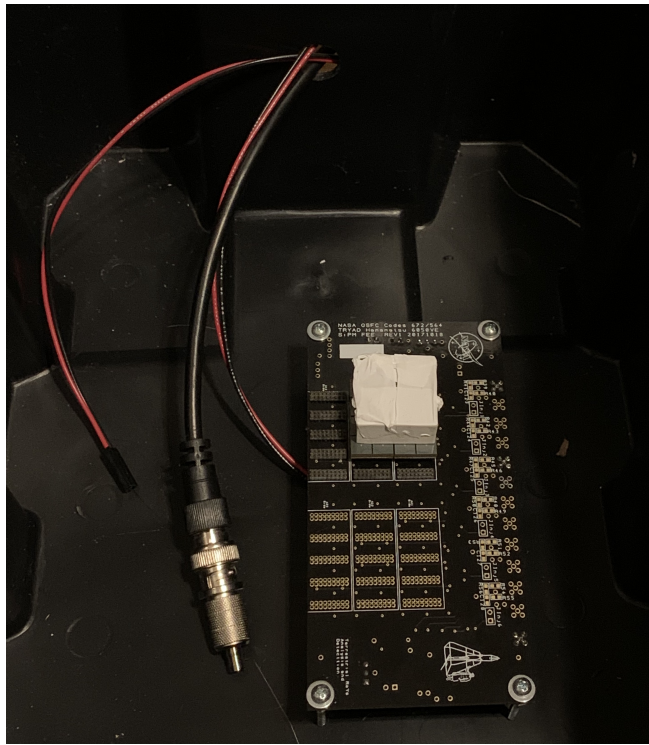


Figure 9: Image of testing setup from interior of light tight box

The scintillators are surrounded by white Teflon tape to retain photons inside the detector and the whole detector apparatus is placed in a black box to prevent photons from outside sources interfering with measurement. The SiPMs are powered at 45V using an outside power supply and the output of the SiPMs are summed and shaped by a separately-powered front-end electronics circuit board. The choice of Hamamatsu SiPMs and front-end electronics was primarily due to prior experience and easy access. The whole detector assembly is placed in a homemade light tight box during testing with signal, bias power, and board power cables

carefully run out of the box with felt coverings. The partially assembled detector in the light tight box is shown in Figure 9.

4 Results

4.1 Experimental design

In order to characterize the design, radiation sources from the Physics Department would be placed on the detector. These sources produce gamma rays ranging in energy from 122 keV to 1333 keV. The response to Cs-137 in particular would be compared to models and other experiments to determine the quality of the detector. This aspect of experimentation is replicated to some degree in MEGAlib simulation, described below. Each scintillator can be characterized individually before being combined into pairs. For each scintillator, a line should be fit to calibrate the energy of incoming gamma rays to the measured voltages. Each calibration requires about four different sources. For each pair of scintillators, the pulses can be discriminated and the resulting measures for each scintillator should match the individual calibrations.

More specifically, the detector circuit board is connected to a constant bias voltage of 45 V, with a separate 3.3 V supply for the board itself. The board must be in the light tight box before providing bias voltage, or the SiPMs risk being damaged by the large number of photons interacting with them. The summed output of the current board design provides the simplest amplification while measuring all of the populated SiPM slots. A SSMB to BNC adapter was obtained to read the output on a fast modern oscilloscope, with a trigger set to identify real pulses and ignore the noise. With one of the radiation sources placed on top of the wrapped scintillator positioned carefully on the SiPMs, voltage pulses should be seen on the oscilloscope. While eventually a range of gamma ray sources will be used for calibration and the various options at Swarthmore are described in Appendix B, a Cesium-137 source is recommended for initial trials.

4.2 Expected results

A real pulse is expected to be on the order of 20-300 mV, though the duration will vary significantly from a few nanoseconds to a few hundred nanoseconds. Experimentation is required to

trigger and then save at least ten thousand pulse waveforms from the oscilloscope. The pulse heights can be measured on the oscilloscope and a live histogram should demonstrate photopeaks and/or Compton edges depending on the scintillator and the energy of the gamma ray source. Post processing of the data can clean up extraneous peaks and allow for background subtraction and comparisons with other trials.

Identifying the voltage measurements for the centers of photopeaks or Compton edges allows for calibrating the detector's voltage measurements to gamma ray energies. In a simple case, such as for Cesium-137, the center of a photopeak appears directly at the equivalent to 662 keV. A Compton edge for the same source would appear at the equivalent to 477 keV. A Gaussian fit to a photopeak allows for calculating the resolution of the detector setup using a full-width half-max calculation. Resolution describes how well the detector can identify and distinguish between similar energies. With fully calibrated and characterized scintillators, the full phoswich detector can be described easily in simulation and tested with multiple sources, including sources with other particles beyond gamma rays.

5 Simulation

In order to investigate the possible capabilities of a gamma ray detector in this size and shape I modeled the scintillators in MEGALib.[14] MEGALib is a powerful wrapper for industry standard particle physics simulator GEANT4.[15] MEGALib is limited, however, as individual pulses cannot be viewed. The results from MEGALib depict the expected distribution of each scintillator's response to a range of radioactive sources, mirroring the planned experimental procedure.

Without my own experimental measurements, values for the energy resolutions (how well a detector system can distinguish between similar energy particles) have been drawn from various sources in published literature. I only selected papers using silicon photomultipliers or similar photodetectors, rather than the older photomultiplier tubes. For standardization, all values were selected for Cesium-137 with 662 keV gamma rays. Improved simulation would require using a consistent range of sources for each scintillator, obtained through experimentation with my particular setup. The energy resolution values, measured by the width of a Gaussian photopeak at half the max, for BGO, 7.8%, and CsI(Tl), 4.8%, are from Moszyński, M. et al.[16] An approximate value for the fast plastic, EJ-212, of 15.8% was obtained from studies on a range

of similar plastics by Eljen Sweany M., et al though the energy resolution for the plastic was obtained from analysis of a Compton edge, rather than a photopeak.[17] Though two types of plastic were purchased from Eljen, only the EJ-212 was simulated as the subtle differences between EJ-212 and EJ-240 were not easily modeled.

An initial MEGAlib simulation of 662 keV gamma rays from a Cesium-137 source interacting with the detector scintillator blocks is shown in Figure 10 below.

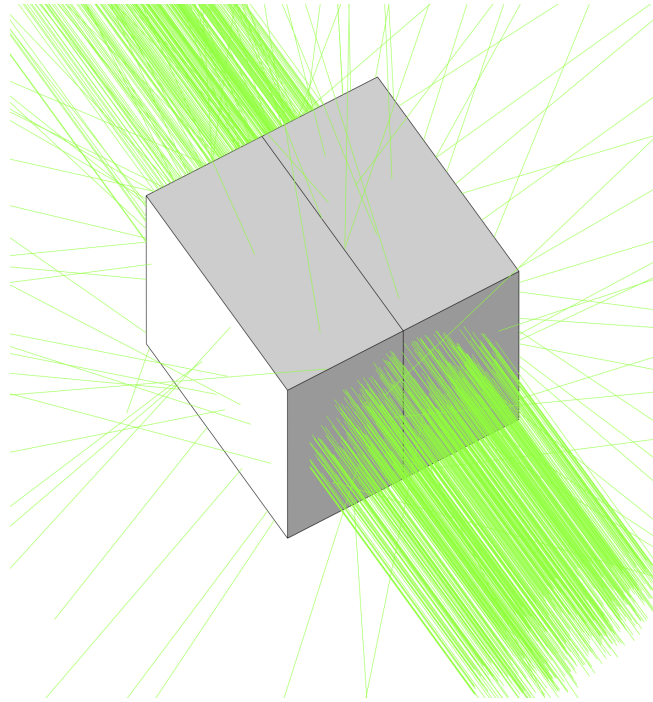


Figure 10: MEGAlib simulation of 661 keV gamma rays interacting with detector

The distribution of energies in an example of combined scintillators is shown in Figure 11, with the majority of the events in the CsI(Tl) crystal scintillator. The distribution does demonstrate the Compton edge at 477 keV and photopeak at 662 keV as anticipated, with the expected 4.8% resolution. As this simulation is based on literature review values, the simulation resolution should remain approximately consistent to the input values. The plastic scintillator emphasizes the Compton scattering interactions, leading to a larger Compton edge than just CsI(Tl). Additionally, the plastic scintillator demonstrated almost no photoeffect interactions as expected. With identically sized scintillators, the crystals consistently outperformed the plastics, though that is to be expected as the higher density crystals will always have more interactions.

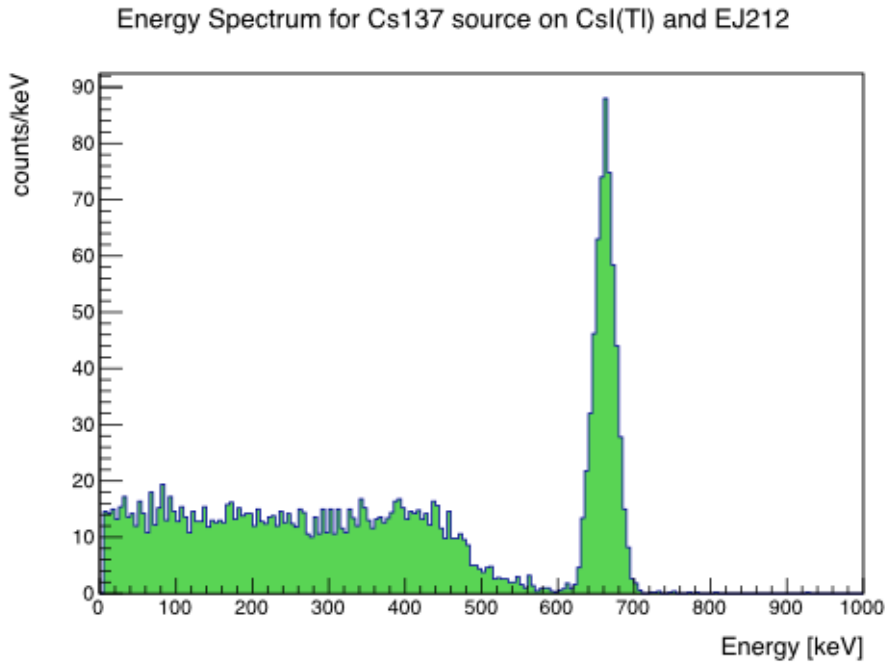


Figure 11: MEGALib simulation energy distribution with CsI(Tl) crystal and EJ212 plastic

6 Conclusion

While experimentation is needed to truly demonstrate feasibility, the initial simulation and literature review results support further research into these small-scale phoswitch gamma ray detectors with silicon photomultipliers. This project should serve as a road-map for extended work using the lab materials and lab protocols described above.

I built a full testing setup with light tight box and various detector configurations, so lab experimentation later in the summer of 2020 or in future years should be a relatively simple process. With experimental data and improved simulations, the optimal combination of scintillator materials should be determined. An expanded project might involve identifying the optimal shape of the scintillator materials using simulations, as in the PhosWatch project.[7] In the longer term, low voltage and small footprint gamma detectors like the phoswitch detector described here will enable secondary instrumentation goals on large satellites or primary instrumentation goals for small satellite projects.

7 Acknowledgements

I am extremely grateful to Professor Lynne Molter for advising me though a very strange semester. Dr. Georgia de Nolfo provided the concept, training, and critical materials to make the project possible. Grant Mitchell helped immensely with MEGALib simulation. At Swarthmore, Professor Hillary Smith kindly provided experimental equipment and Edmond Jaoudi and Cassy Burnett assisted with obtaining other materials.

References

- [1] Mike Fogle et al. “Terrestrial RaYs Analysis and Detection (TRYAD) Cubesat Mission”. In: *Proceedings of the 31st Annual AIAA/USU Conference on Small Satellites* (2017). URL: <https://digitalcommons.usu.edu/smallsat/2017/all2017/36/>.
- [2] S. N. Axani, K. Frankiewicz, and J. M. Conrad. “The CosmicWatch Desktop Muon Detector: A self-contained, pocket sized particle detector”. In: *Journal of Instrumentation* 13.3 (2018). ISSN: 17480221. DOI: 10.1088/1748-0221/13/03/P03019.
- [3] James E. Parks. *The Compton Effect – Compton Scattering and Gamma Ray Spectroscopy*. Tech. rep. University of Tennessee, Department of Physics and Astronomy, 2015, pp. 1–37. URL: <http://www.phys.utk.edu/labs/modphys/Compton%20Scattering%20Experiment.pdf>.
- [4] W. Hennig et al. “Digital pulse shape analysis with phoswitch detectors to simplify coincidence measurements of radioactive Xenon”. In: *27th Seismic Research Review: Ground-Based Nuclear Explosion Monitoring Technologies*. 2005, pp. 787–794.
- [5] Z. Gu et al. “A DOI detector with crystal scatter identification capability for high sensitivity and high spatial resolution PET imaging”. In: *IEEE Transactions on Nuclear Science* (2015). ISSN: 00189499. DOI: 10.1109/TNS.2015.2408333.
- [6] E. Costa, E. Massaro, and L. Piro. “A BGO-CsI(Ti) Phoswitch: A new detector for X- and gamma-ray astronomy”. In: *Nuclear Instruments and Methods in Physics Research* 243.1986 (1985), pp. 572–577.

- [7] W. Zhang et al. “An optimized design of single-channel beta-gamma coincidence phoswich detector by Geant4 Monte Carlo simulations”. In: *Science and Technology of Nuclear Installations* 2011 (2011). ISSN: 16876075. DOI: 10.1155/2011/741396.
- [8] W. Hennig et al. “Development of a phoswich detector for radioxenon field measurements”. In: *IEEE Transactions on Nuclear Science* 61.5 (2014), pp. 2778–2785. ISSN: 00189499. DOI: 10.1109/TNS.2014.2343158.
- [9] Lukas Middendorf. “Data acquisition for an SiPM based muon detector”. In: (2018), p. 202. DOI: 10.18154/RWTH-2018-225274. URL: <http://inspirehep.net/record/1775673>.
- [10] P. Mekarski et al. “Monte Carlo simulation of a PhosWatch detector using Geant4 for xenon isotope beta-gamma coincidence spectrum profile and detection efficiency calculations”. In: *Applied Radiation and Isotopes* 67.10 (2009), pp. 1957–1963. ISSN: 09698043. DOI: 10.1016/j.apradiso.2009.07.005. URL: <http://dx.doi.org/10.1016/j.apradiso.2009.07.005>.
- [11] Parviz Ghorbani et al. “Experimental study of a large plastic scintillator response with different reflective coverings based on digital pulse processing method”. In: *Journal of Radioanalytical and Nuclear Chemistry* 321.2 (2019), pp. 481–488. ISSN: 15882780. DOI: 10.1007/s10967-019-06596-5. URL: <https://doi.org/10.1007/s10967-019-06596-5>.
- [12] Olivier Girard et al. “Characterisation of silicon photomultipliers based on statistical analysis of pulse-shape and time distributions”. In: (2018). URL: <http://arxiv.org/abs/1808.05775>.
- [13] L. Varga. “Characterization and optimization of Silicon Photomultipliers and small size scintillator tiles for future calorimeter applications”. PhD thesis. Eötvös Loránd University, HU, 2017.
- [14] A. Zoglauer, R. Andritschke, and F. Schopper. *MEGALib - The Medium Energy Gamma-ray Astronomy Library*. 2006. DOI: 10.1016/j.newar.2006.06.049.
- [15] S. Agostinelli et al. “GEANT4 - A simulation toolkit”. In: *Nuclear Instruments and Methods in Physics Research, Section A: Accelerators, Spectrometers, Detectors and Associated Equipment* 506.3 (July 2003), pp. 250–303. ISSN: 01689002. DOI: 10.1016/S0168-

9002(03)01368-8. URL: <https://www.sciencedirect.com/science/article/pii/S0168900203013688>.

- [16] M. Moszyński et al. “Energy resolution of scintillation detectors readout with large area avalanche photodiodes and photomultipliers”. In: *IEEE Transactions on Nuclear Science* 45.3 PART 1 (1998), pp. 472–477. ISSN: 00189499. DOI: 10.1109/23.682429.
- [17] M. Sweany et al. “Interaction position, time, and energy resolution in organic scintillator bars with dual-ended readout”. In: *Nuclear Instruments and Methods in Physics Research, Section A: Accelerators, Spectrometers, Detectors and Associated Equipment* 927 (2019), pp. 451–462. ISSN: 01689002. DOI: 10.1016/j.nima.2019.02.063.

Appendices

A Materials

A.1 Cost

The final bill of materials can be found in the next section. The total cost was \$2,336.00, dominated by \$1,296.00 for 16 Hamamatsu SiPMs. Scintillators from Ejen and Proteus-PP made up the majority of the remaining costs. The Eljen EJ-212 is the fastest response scintillator, followed by the Eljen EJ-240. The Proteus-PP crystal scintillators, CsI(Tl) and BGO, both have long response times.

A.2 Bill of Materials

Item	Description	Dimensions	Manufacturer	Unit Price	Units	Line Price
Polished CsI(Tl)	All sides polished crystal, hygroscopic	24mm x 24mm x 12mm	Proteus-PP	\$150.00	1	\$150.00
Polished BGO	All sides polished crystal	24mm x 24mm x 12mm	Proteus-PP	\$300.00	1	\$300.00
EJ-240 Plastic	Clear plastic	24mm x 24mm x 12mm	Eljen	\$176.00	1	\$176.00
EJ-212 Plastic	Clear plastic	24mm x 24mm x 12mm	Eljen	\$174.00	1	\$174.00
S16150-6050HS	Silicon Photomultipliers	6mm x 6mm x 6mm	Hamamatsu	\$81.00	16	\$1,296.00
SiPM mounts	8 pin mount for two SiPMs each	6 mm x 12 mm x 6 mm	NASA GSFC	\$0.00	8	\$0.00
SiPM circuit board	Readout and signal shaping board	approx. 2in. x 4in.	NASA GSFC	\$0.00	1	\$0.00
Teflon Tape	Simple roll of Teflon tape	1/2 in. x 260 in.	Home Depot	\$1	1	\$1.00
BNC Adapter	SSMB to BNC Adapter, price from Ed	12mm x 12mm x 25 mm		\$100	1	\$100.00
Delivery	Estimate			\$100	1	\$100.00
Black plastic box	Thick black plastic storage box with lid		Home Depot	\$20.00	1	\$20.00
Black "flock" paper	#40, 27" x 36", 2 Sheets, Non-Adhesive	27" x 36"	Edmund Optics	\$19.00	1	\$19.00
					Total Price	\$2,336.00

B Radiation sources

A list of the gamma ray sources made available from the Swarthmore Physics Department is provided below along with their expected gamma ray energies. Calibration of each scintillator for low and medium energy gamma rays would require using a range of energies from around 100 keV to about 1.2 MeV. Gamma energies were obtained from Stanford's Environmental Health and Safety database.

Sources	Gamma Energies	Peak Energy in keV
Co-57	0.014 MeV (9.54 %) 0.122 MeV (85.6 %) 0.136 MeV (10.6 %) 0.692 MeV (0.02 %)	122 keV
Co-60	1.1732 MeV (99.90 %) 1.3325 MeV (99.98 %)	1173 keV, 1333 keV
Cd-109	0.088 MeV (4%), 0.025 MeV (18 %), 0.022 MeV (84%) [xrays]	
Mn-54	0.835 MeV (100 %)	835 keV
Cs-137	0.662 MeV (85 %)	662 keV
Na-22	0.511 MeV, 1.275 MeV	1275 keV
Ba-133	.035 MeV (22.6%), .081 MeV (34%), .276 MeV (7%), .303 MeV (18%), .356 MeV (62%), .383 MeV (9%)	356 keV, 303 keV

C MEGAlib Code

Written for MEGAlib v3.00, this code can be run after installing the MEGAlib packages from <http://megalibtoolkit.com/setup.html> A very useful example of data analysis can be found <http://megalibtoolkit.com/documentation.html>

C.1 MEGAlib Geometry file

```
// Geometry Setup for simple block detector
// 24mm x 24mm x 12mm block of scintillator on 16 6mm x 6mm SiPMs
// saved as blockgeo.geo.setup

// Global Parameters
Name SimpleBlock
Version 1.0

Include $(MEGALIB)/resource/examples/geomega/materials/Materials.geo

// sphere is 3cm radius , centered on 0,0,0
SurroundingSphere 20.0, 0.0, 0.0, 0.0, 20.0
```

//----- Materials -----

Material CsITl

CsITl.Density 4.51

CsITl.ComponentByAtoms Cs 1

CsITl.ComponentByAtoms I 1

Material BGO2

BGO2.Density 7.13

BGO2.ComponentByAtoms Bi 4

BGO2.ComponentByAtoms Ge 3

BGO2.ComponentByAtoms O 12

Material EJ212

EJ212.Density 1.023

EJ212.ComponentByAtoms C 9

EJ212.ComponentByAtoms H 10

Material EJ240

EJ240.Density 1.023

EJ240.ComponentByAtoms C 9

EJ240.ComponentByAtoms H 10

Echo Materials Loaded

//----- Volumes -----

Volume World_Volume

World_Volume.Shape BOX 10 10 10

World_Volume.Material Vacuum

World_Volume.Visibility 1

World_Volume.Color 0

World_Volume.Mother 0

#Volume BGO_Box

#BGO_Box.Material BGO2

#BGO_Box.Shape BOX 1.2 1.2 0.6

#BGO_Box.Position 0 0 0.6

#BGO_Box.Visibility 1

#BGO_Box.Color 1

#BGO_Box.Mother World_Volume

Volume EJ_Box

EJ_Box.Material EJ212

EJ_Box.Shape BOX 1.2 1.2 0.6

EJ_Box.Position 0 0 -0.6

EJ_Box.Visibility 1

EJ_Box.Color 2

EJ_Box.Mother World_Volume

Volume CsITl_Box

CsITl_Box.Material CsITl

CsITl_Box.Shape BOX 1.2 1.2 0.6

CsITl_Box.Position 0 0 0.6

CsITl_Box.Visibility 1

CsITl_Box.Color 3

CsITl_Box.Mother World_Volume

Echo Volumes Loaded

//----- Detectors -----

#Scintillator BGO_Scint

#BGO_Scint.SensitiveVolume BGO_Box

#BGO_Scint.DetectorVolume BGO_Box

#BGO_Scint.TriggerThreshold 5

#BGO_Scint.NoiseThreshold 5

#BGO_Scint.EnergyResolution Gauss 662.0 662.0 23.2

#BGO_Scint.EnergyResolution Gauss 511.0 511.0 17.9

Scintillator CsITl_Scint

CsITl_Scint.SensitiveVolume CsITl_Box

CsITl_Scint.DetectorVolume CsITl_Box

CsITl_Scint.TriggerThreshold 5

CsITl_Scint.NoiseThreshold 5

CsITl_Scint.EnergyResolution Gauss 662.0 662.0 14.3

CsITl_Scint.EnergyResolution Gauss 511.0 511.0 11.02

Scintillator EJ_Scint

EJ_Scint.SensitiveVolume EJ_Box

EJ_Scint.DetectorVolume EJ_Box

EJ_Scint.TriggerThreshold 5

EJ_Scint.NoiseThreshold 5

EJ_Scint.EnergyResolution Gauss 478.0 478.0 75.5

EJ_Scint.EnergyResolution Gauss 340.0 340.0 49.3

Echo Detectors loaded

//----- Triggers -----

#Trigger BGO-Trig

#BGO-Trig.TriggerByChannel true

```
#BGO_Trig.Detector BGO_Scint 1
```

```
Trigger CsITl_Trig
```

```
CsITl_Trig.TriggerByChannel true
```

```
CsITl_Trig.Detector CsITl_Scint 1
```

```
Trigger EJ_Trig
```

```
EJ_Trig.TriggerByChannel true
```

```
EJ_Trig.Detector EJ_Scint 1
```

```
Echo Triggers Loaded
```

C.2 MEGAlib Source file

```
// Simulation Setup for simple block detector
```

```
// 24mm x 24mm x 12mm block of scintillator on 16 6mm x 6mm SiPMs
```

```
// saved as blocktest.source
```

```
// Global Parameters
```

```
Name SimpleTest
```

```
Version 1.0
```

```
Geometry ./blockgeo.geo.setup
```

```
//----- Simulation Options -----
```

```
DefaultRangeCut 0.001
```

```
PhysicsListEM Livermore
```

```
PhysicsListHD qgsp-bert-hp
```

```
StoreSimulationInfo all
```

StoreCalibrated true

StoreSimulationInfoIonization true

DiscretizeHits true

//----- Run Options -----

Run Cs137Beam

Cs137Beam.FileName Cesium137Beam-CsIT1-EJ212

Cs137Beam.Triggers 10000

Cs137Beam.Source Cs137

Cs137.ParticleType 1

Cs137.Spectrum Mono 662.0

Cs137.Beam HomogeneousBeam 4.0 0.0 0.0 -1.0 0.0 0.0 1.0

Cs137.Flux 1000.0